ON SOLAR TYPE PROTOSTARS

Karl-Heinz A. Winkler
Lawrence Livermore Lab, Los Alamos Scientific Lab, and
Max-Planck-Institut für Physik und Astrophysik

Michael J. Newman
Los Alamos Scientific Laboratory

The formation of a 1 $M_\odot$ protostar in spherical symmetry has been followed in time dependent hydrodynamics with a detailed description of the equation of state and a careful treatment of radiative transport. The comparison of the dynamic evolution with observation is made in terms of the Hertzprung-Russell diagram. It is found that the evolution following from Larson's initial condition produces quantitatively and qualitatively better agreement than that following from the initial condition of Hayashi, including the first appearance of the object as an infrared source. Of particular importance for a correct physical understanding of the formation process is an adequate description of the accretion shock. Pressure ionization and electron degeneracy effects are of increasing importance for the internal structure of lower mass objects.

In recent years the computational difficulties which led Hayashi and his coworkers to adopt rather unnatural starting conditions for their early studies of star formation have been largely overcome, and it has become possible, at least in spherical symmetry, to follow in some detail the hydrodynamic collapse and accretion of an initially tenuous interstellar cloud from the onset of the first Jeans gravitational collapse all the way to the stellar state. The differences in early pre-main sequence evolution resulting from the latter type of initial condition, first investigated in detail by Larson, have been discussed by Newman and Winkler (1980). In the present paper we discuss briefly the essential microscopic physics necessary for a successful calculation of star formation beginning from Larson's initial condition, the resolution which must be afforded the stellar atmosphere and the strong accretion shock to obtain a physically correct description of the evolution, and present a comparison of observations of young stars with the evolutionary tracks predicted by the one-dimensional hydrodynamic calculations.

The thermodynamic detail required in a correct description of the state of a protostellar core during the late stages of the

Space Science Reviews **27** (1980) 261–266. 0038–6308/80/0273–261 $00.90.

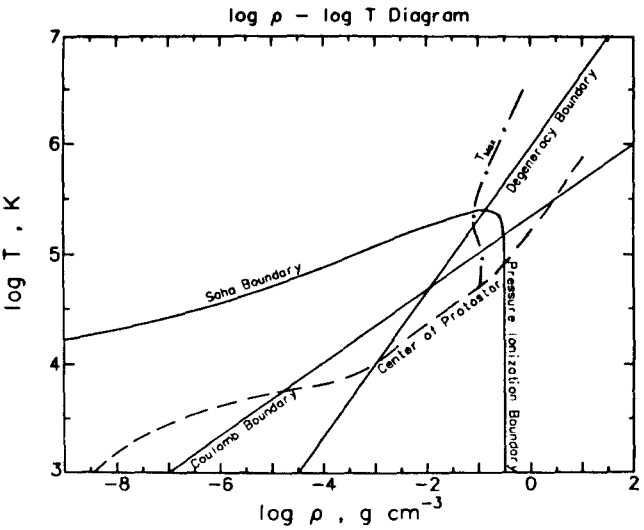

Fig. 1. - Thermodynamic processes. The Saha and pressure ionization boundaries, the Coulomb effect boundary, and the degeneracy boundary for a free electron gas are shown, with the tracks of the center of a 1 $M_\odot$ protostar and the off-center temperature maximum.

formation process has been discussed by Winkler and Newman (1980b). In Fig. 1 we see the track in the density-temperature diagram of the center of a protostar of 1 $M_\odot$, and of the off-center temperature maximum which develops under the combined influence of pressure ionization and electron degeneracy. The density of the collapsing interstellar cloud increases considerably faster than its temperature, and Coulomb corrections to the equation of state become important before the material is ionized by temperature effects. Prior to ionization, conditions of density and temperature are reached at which free electrons would become degenerate, and the central regions of the core become slightly electron degenerate as the material is pressure ionized. The material near the off-center temperature maximum leaves the degenerate zone and crosses the Saha boundary to be ionized by temperature effects. It has reached the radial track of the present sun by the time the calculation is terminated with 99% of the mass assembled in the core. The central region must undergo further contraction and heating before achieving conditions characteristic of a mature main sequence star.

Some attention to microscopic detail is also required for an adequate description of the envelope structure. In the method of Tscharnuter and Winkler (1979) the moments of the radiation field are determined from the time-dependent transport equation of Castor (1972) with variable Eddington factor f. Winkler and Newman (1980b) included a detailed prescription for gas and dust opacities, and found the behavior shown in Fig. 2. The luminosity during the main accretion phase is produced in the very narrow shock front and remains nearly constant throughout the envelope. In regions of high opacity the radiation is effectively absorbed and re-emitted, the optical depth is high, the radiation field is nearly isotropic, and the Eddington factor is near 1/3. Under these conditions the diffusion approximation, which has been used extensively in previous

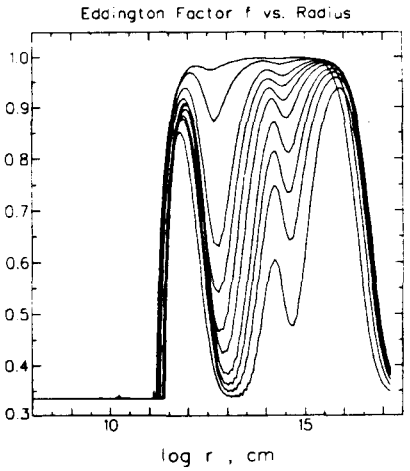

Fig. 2. - Eddington factor f vs. radius. The ratio f=K/J of the radiation pressure to energy density of the radiation field is shown when 10, 20, 30, 40, 50, 60, 70, 80, 90, and 99 percent of the material has been assembled in the stellar core.

star formation calculations, is not a bad description of the flow. However, in the low-opacity region just outside the shock, and throughout the envelope in late stages of the accretion as the envelope is depleted of material, the efficiency of absorption is low, the radiation field becomes increasingly anisotropic as it is peaked in the forward direction away from the shock front, and the Eddington factor approaches unity. The presence of embedded regions of locally low opacity during the initial high-density-envelope phase makes constant f=1/3 a poor approximation, and constant f=1 is a reasonable description only for late times in the envelope. It is clear that the diffusion approximation with Eddington factor constant in time and space cannot offer a realistic treatment of envelope structure for protostar calculations.

Early calculations of the evolution of a slightly Jeans unstable interstellar cloud of 1 $M_\odot$ have been reviewed by Winkler and Newman (1980a), who critically discussed the various numerical techniques applied. It was found that many of the discrepancies appearing in the literature were the result of problems in the treatment of the strong accretion shock, whose structure in the present calculation is shown in Fig. 3. In panel (a) we see the very steep density decrease of some 12 orders of magnitude occuring at the edge of the stellar core, and in panel (b) the very sharp deceleration of the free falling envelope material as it encounters the core. Here each individual grid point of the calculation is plotted separately, and we note the excellent resolution afforded by the use of the freely moving coordinate system as these very steep structures evolve in both mass and spatial position. In panel (c) the edge of the core is very sharply defined by the maximum of the slope $|d\ln\rho/d\ln r|$ of the density drop, and the position of the shock front, which has been only slightly smeared out by the use of artificial viscosity, is also well defined as the maximum in the viscous energy generation rate

https://doi.org/10.1017/S025292110008163X Published online by Cambridge University Press

ε_Q/ρ. Also shown is the profile of the luminosity which is produced primarily in the inner portion of the shock. In panel (d) we see the gas temperature (crosses) and radiation temperature (squares), and note that they are out of equilibrium in the accretion shock as well as in the optically thin, essentially adiabatic preheating compression zone in front of the shock. The luminosity produced in the preheating zone is negligible compared to that produced in the temperature overshoot relaxation zone, in good agreement with the assumptions of Larson, as discussed by Winkler and Newman (1980a).

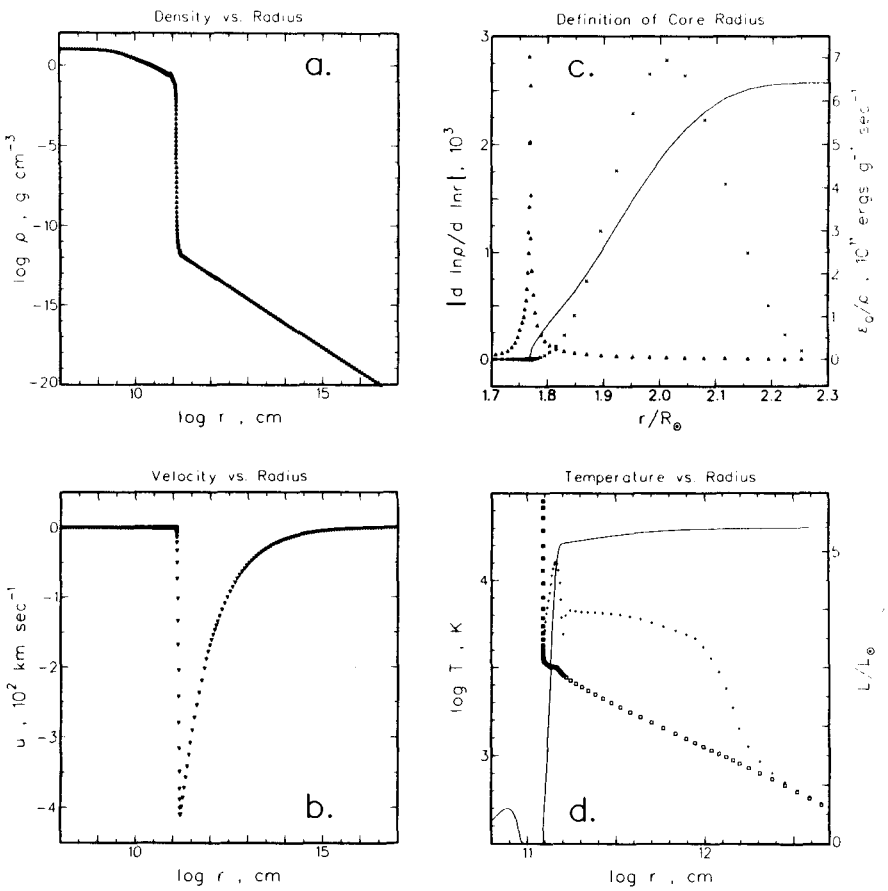

Fig. 3. - Shock front structure late in the main accretion stage. a) Density vs. radius. b) Velocity vs. radius. c) Definition of the core radius. The slope $|d\ln\rho/d\ln r|$ of the atmospheric density drop (triangles, left scale), the rate of viscous energy generation ε_Q/ρ (crosses, right scale), and the luminosity profile (solid curve, arbitrary scale) are shown as a function of radius. d) Temperature vs. radius. The gas (crosses) and radiation (squares) temperatures are presented (left scale). The luminosity profile from panel c) is replotted logarithmically (right scale).

https://doi.org/10.1017/S025292110008163X Published online by Cambridge University Press

In Figure 4 the clusters of young stars in Taurus-Auriga, Orion, NGC 2264, and NGC 7000/IC 5070 from Cohen and Kuhi (1979) are superimposed in a composite Hertzsprung-Russell diagram. Also shown are the Zero-Age Main Sequence, the 1 $M_\odot$ Hayashi track, and the evolutionary path of Winkler and Newman (1980a). In the latter calculation the effective temperature suddenly increases and the protostar moves abruptly to the left in the diagram when 96% of the material has been accreted by the core and the material outside the shock front becomes optically thin to radiation. Prior to this point in the evolution the object essentially appears as an infrared source. Curves of this shape can account for the objects occupying the upper lefthand corner of the diagram as stars only slightly more massive than the sun, while fully convective stars of such high effective temperature and luminosity must be quite massive and therefore fairly rare. Dynamic evolution parrallel to the main sequence would occur at somewhat larger radius if convective energy transport and the scouring out of light thermonuclear fuels were included in the calculation, in good agreement with the diagonal clustering of the observed young stars.

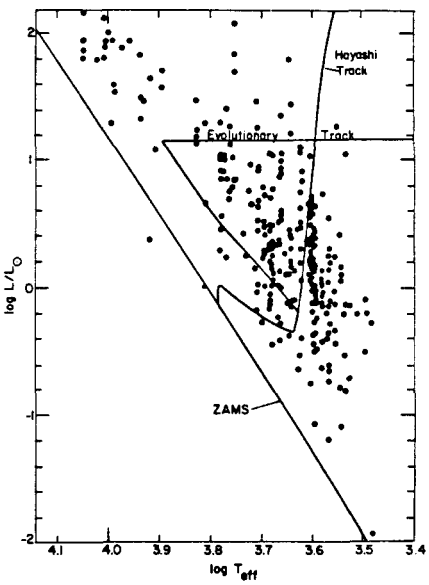

Fig. 4. - Comparison with observations. The position in the Hertzsprung-Russell diagram of young stars from Cohen and Kuhi are shown, with the Zero-Age Main Sequence, the 1 $M_\odot$ Hayashi track, and the dynamic track of a solar-type protostar.

REFERENCES:

Castor, J. 1972, Ap. J., 178, 779.
Cohen, M., and Kuhi, L. V. 1979, Ap. J., 41, 743.
Newman, M. J. and Winkler, K.-H. A. 1980, Proceedings of the Lunar and Planetary Institute Topical Conference on the Ancient Sun (in press).
Tscharnuter, W., and Winkler, K.-H. A. 1979, Computer Phys. Comm., 18, 171.
Winkler, K.-H. A., and Newman, M. J. 1980a, Ap. J., 236, 201.
Winkler, K.-H. A., and Newman, M. J. 1980b, Ap. J., 238, 311.

DISCUSSION

COLGATE: What is the optical thickness of the shell of dust from where it is evaporated to infinity? Where is the photosphere?

WINKLER: At the beginning of the accretion phase it is 80-100, and when 5% of the mass is in the core it is 30. The photosphere is at 10^{15} cm at first and then it decreases to the shock front or corona as matter falls on the core.

A. COX: Did Kuhi intend to use the data in your H-R diagram to verify the Hayashi tracks? Do the data verify yours?

WINKLER: Kuhi did not actually use the data to verify the Hayashi tracks. When 5% of the matter is left in the envelope at the very end of the accretion phase all the rest of the evolution is in this part of the H-R diagram. I don't see any contradiction with the data, but the Hayashi tracks would display an infrared appearance first.

A. COX: What happens for different masses? Are all the observed stars supposed to have 1 $M_\odot$?

WINKLER: They would have masses 1-3 $M_\odot$.

https://doi.org/10.1017/S025292110008163X Published online by Cambridge University Press